Asymmetric Catalysis | Hot Paper |

Crossed Regio- and Enantioselective Iron-Catalyzed [4+2]-Cycloadditions of Unactivated Dienes

Elena Braconi and Nicolai Cramer*

Abstract: *The cyclohexene motif is ubiquitous in nature and specialty chemicals. A straightforward selective access to chiral cyclohexenes from unactivated dienes and dienophiles is not feasible by classical Diels–Alder reaction and constitutes an unsolved synthetic challenge. We report a mild and enantioselective iron-catalyzed cross-[4+2]-cycloaddition of unactivated dienes providing access to chiral 1,3-substituted vinylcyclohexenes. The development of bis-dihydroisoquinoline ligands was vital to obtain iron complexes that display high reactivities and excellent chemo-, regio- and enantioselectivities towards the targeted cyclohexenes. A range of diene substrates is well accommodated including feedstocks like butadiene, isoprene and myrcene. The structures of different iron complexes are mapped by X-ray crystallographic analysis and linked to their performance.*

Chiral cyclohexenes bearing vinyl substituents are the structural core of numerous natural products,[1] such as (*R*)-limonene,[2] aucantene[3] and diclausenans A/B[4] (Scheme 1A). Among the different strategies to forge the cyclohexene ring,[5–8] the Diels–Alder [4+2]-cycloaddition[9] is one of the most efficient and straightforward approaches (Scheme 1B). The presence of activated dienes and/or dienophiles, bearing electron-donating or electron-withdrawing groups, is a prerequisite for reactivity,[10] regio-[11] as well as enantioselectivity.[12] These requirements make the Diels–Alder reaction unsuitable for selectively accessing unfunctionalized cyclohexenes from unbiased precursors.

Transition metal-catalyzed [4+2]-cycloadditions[13] can accommodate non-polarized substrates by coordinating to their pi-bonds.[14,15] The use of unactivated alkenes as "dienophile" component is limited to intramolecular Rh-catalyzed [4+2]-cycloadditions.[16,17] Reactivity and selectivity are strongly substrate dependent and attempts to develop asymmetric versions only resulted in moderate levels of
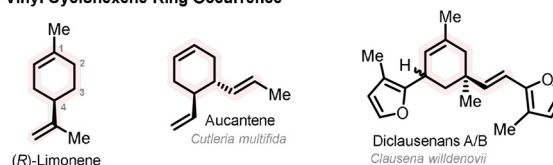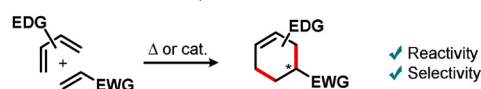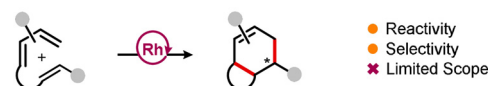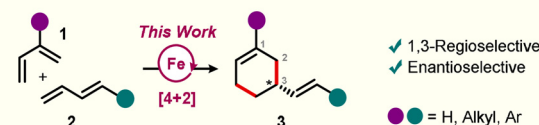
Scheme 1. Occurrence and synthetic approaches to cyclohexenes.

enantiocontrol. Therefore, straightforward and enantioselective access to unbiased cyclohexenes remains an unsolved synthetic challenge,[18,19] making the development of efficient catalysts to access this valuable scaffold of significant importance.

The application of Earth-abundant metals such as iron[20–22] in catalysis is highly desirable due to their high availability, low price and low toxicity. Diimine iron-complexes are particularly attractive due to their ability to catalyze a variety of reactions, such as olefin polymerization,[23] hydrofunctionalization[24] and cycloadditions.[25–28] The diimine ligand precursors are easily accessible and modular in nature, allowing facile tuning of the steric and electronic properties of the corresponding iron complexes.

We herein report an enantioselective iron-catalyzed cross-[4+2]-cycloaddition of unactivated branched and linear dienes to access a broad scope of 1,3-substituted vinylcyclohexenes in excellent yields and enantioselectivity (Scheme 1C). Natural vinyl-cyclohexenes such as limonene possess a 1,4-substitution pattern. They can be sourced from nature and used for chiral pool strategies.[29] The presented synthetic method is complementary, enabling a unique approach to the less accessible 1,3-substituted analogs.

We have recently reported a chiral α-diimine iron catalyst class enabling the enantioselective cross-[4+4]-cycloaddition

[*] E. Braconi, Prof. Dr. N. Cramer
Institute of Chemical Sciences and Engineering (ISIC), EPFL SB ISIC
LCSA, BCH 4305
1015 Lausanne (Switzerland)
E-mail: nicolai.cramer@epfl.ch
Homepage: https://www.epfl.ch/labs/lcsa/

of alkyl-substituted 1,3-dienes to cyclooctadienes.[28] Along the same lines, Chirik reported exclusive access to aryl-substituted [4+4]-cycloadducts with a pyridine-imine (PI) iron catalyst.[27] In a follow-up, we were wondering if selective formation of cross-[4+2]-cycloadduct **3** over the competing [4+4]-product as well as linear isomers and oligomers could be triggered by catalyst/ ligand tuning.

We started investigating the asymmetric iron-catalyzed cross-[4+2]-cycloaddition between 2-methylenebut-3-en-1-yl)benzene (**1a**) and (*E*)-buta-1,3-dien-1-ylbenzene (**2a**) as model substrate combination (Table 1). The iron(II) complexes were conveniently in situ reductively activated by Bu₂Mg.[30] Chiral α-diimine catalyst **Fe1** (R = H, R¹ = Cy) promoted full conversion of **1a** and **2a** under very mild conditions and with excellent chemo- and regioselectivity. Cyclohexene **3aa** was obtained in 90 % yield and promising 68:32 er (entry 1). Increasing the catalyst backbone size (**Fe2**,

R = Me) improved the enantioselectivity of **3aa** to 76:24 er (entry 2). However, **Fe3** having slightly bulkier substituents (R = Et) affected detrimentally chemo- and enantioselectivity (entry 3). In contrast, progressively increasing the size of the catalyst side-arms had beneficial effects (entries 4,5). Catalyst **Fe5** (R¹ = CMe₂*i*Pr) was the best of this series giving **3aa** in 99 % yield and 83:17 er. Reducing the reaction temperature to −10 °C additionally boosted the selectivity of **3aa** to 96:4 er, while maintaining full conversion and 96 % yield (entry 6). The tipping point was reached with a further increase in the side-arms size (**Fe6**, R¹ = CMe₂*t*Bu), causing a sharp drop of all the reaction parameters (entry 7). When testing catalyst **Fe5** for a diene combination with both substrates having aryl substituents (buta-1,3-dien-2-ylbenzene **1b** and **2a**) cyclohexene **3ba** was still chemoselectively obtained in 83 % yield (entry 8). However, **3ba** was formed in only 61:39 er. The enantiocontrol was virtually lost when **Fe1** was employed as catalyst (entry 9). An increase in the catalyst backbone size (**Fe2**) improved the enantioselectivity of **3ba** to 88:12 er, but coming short at the chemoselectivity end (entry 10), as triene **5ba** was formed as main side-product.

Aiming for a general methodology to access unactivated vinyl-cyclohexenes **3**, the necessity of a different ligand design was apparent. We hypothesized that the increased rigidity of tethering ligand backbone and side-arms may result in improved selectivities. In this respect, we envisioned that a chiral *bis*-dihydroisoquinoline scaffold, previously employed as synthetic intermediate for NHCs[31] and diazaphospholanes,[32] could be used as diimine ligand platform. In this respect, second generation catalyst (*S*,*S*)-**Fe7** equipped with cyclohexyl side-arms provided a convincing performance (entry 11). Not only the [4+2]-chemoselectivity was restored yielding 80 % of **3ba**, but as well giving it in 91:9 er. The enantiomeric ratio could be improved to 92:8 by lowering the reaction temperature to −10 °C (entry 12). Catalyst **Fe8** (R¹ = *i*Pr) displayed a slightly lower selectivity (entry 13). For this series, the tipping point of bulk was reached with **Fe9** (R¹ = *t*Bu), resulting in no product formation with a virtually complete recovery of **1b** and **2a** (entry 14). Notably, second generation *bis*-dihydroisoquinoline-based catalyst **Fe7** shows broader substrate tolerance as it also promotes the formation of cyclohexene **3aa** in 90 % yield and 95:5 er (entry 15).

A comparison of X-ray crystal structures[30] and binding pocket steric maps[33] of catalysts **Fe7–9** with **Fe5** revealed notable differences (Figure 1). For instance, according to the buried volumes (%V_{bur}), **Fe5** (47.6 %) features a more congested catalytic pocket than **Fe7** (43.8 %). **Fe5** shows a relatively symmetric sterically hindered western (W) and eastern (E) hemispheres. **Fe7** displays its main steric bulk over the SW and NE quadrants. Although having very similar buried volumes, the lower enantiocontrol provided by **Fe8** vs. **Fe7** may be related to minor changes at the catalyst active site. The enhanced steric congestion at the binding pocket of **Fe9** (%V_{bur} = 48.8 %) correlates with its very poor catalytic performance. The nature of the ligand side-arms (R¹) has an impact on the torsion angle (θ)[34] of the *bis*-dihydroisoquinoline backbone (θ = 35.15° **Fe7**; θ = 37.84° **Fe8**, θ = 51.58° **Fe9**), plausibly influencing the shielding ability and selectivity of the corresponding iron complexes.

Table 1: Optimization of the asymmetric Fe-catalyzed cross-[4+2]-cycloaddition.

Entry	Fe#	Product	Conv. [%][a]	Yield [%][a]	er[b]
1	Fe1	3 aa	> 95	90	68:32
2	Fe2	3 aa	> 95	75	76:24
3	Fe3	3 aa	80	37	69:31
4	Fe4	3 aa	> 95	99	81:19
5	Fe5	3 aa	> 95	99	83:17
6[c]	Fe5	3 aa	> 95	96	96: 4
7	Fe6	3 aa	88	53	73:27
8	Fe5	3 ba	> 95	83	61:39
9	Fe1	3 ba	> 95	92	51:49
10[d]	Fe2	3 ba	> 95	31	88:12
11[e]	Fe7[e]	3 ba	> 95	80	91: 9
12[c]	Fe7[e]	3 ba	> 95	80	92: 8
13[c]	Fe8	3 ba	> 95	82	12:88
14[c]	Fe9	3 ba	< 5	-	-
15[c]	Fe7[e]	3 aa	> 95	90	5:95

Conditions: 0.33 mmol **1**, 0.3 mmol **2a**, 6 µmol (*R*,*R*)-**Fe#**, 24 µmol Bu₂Mg (1 M in heptane) at 25 °C for 16 h. [a] Determined by ¹H-NMR using 1,2-dichloroethane as internal standard. [b] Determined by chiral HPLC. [c] At −10 °C. [d] **5 ba** was formed as major side-product. [e] (*S*,*S*)-**Fe7** was used.
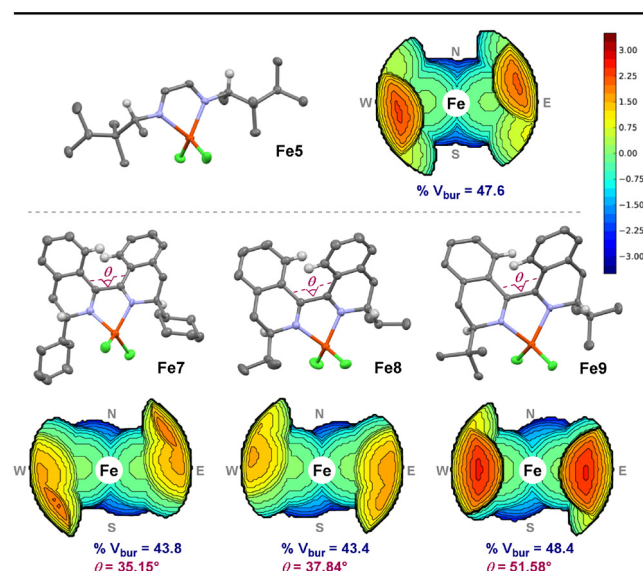
Figure 1. X-ray crystal structures of **Fe5** and **Fe7**–**Fe9**, and corresponding steric maps, buried volumes and torsion angles. Bond radii scaled by 1.17, sphere radius: 3.5 Å, mesh spacing: 0.1 Å.

With optimal catalysts **Fe5** and **Fe7**, the scope of the cross-[4+2]-cycloaddition was explored next (Scheme 2). Aryl-substituted linear dienes equipped with both electron-donating (**2b**–**2c**,**2g**) and electron-withdrawing functionalities (**2d**–**2f**) reacted well in the presence of catalyst (*R*,*R*)-**Fe5**,

yielding cyclohexenes **3ab**–**3ag** in generally good yields and enantioselectivities up to 96:4. Typically, slightly higher enantiomeric ratios were observed for linear dienes bearing electron-withdrawing substituents at the aryl moiety. The absolute configuration of **3ag** (obtained with (*R*,*R*)-**Fe5**) was found to be (*R*) by X-ray structural analysis.[30] Catalyst (*S*,*S*)-**Fe7** displayed a better catalytic performance for the cycloaddition of non-aryl-substituted linear dienes (**2h**–**2i**) with branched diene **1b**. For example, cyclohexene **3bh**, deriving from 1,3-pentadiene, was obtained in 96:4 er. Moreover, branched dienes bearing non-coupled heteroaromatics (**1e**, **1f**), protected alcohols (**1g**), as well as additional peripheral double bonds (**1h**), smoothly engaged in the cross-[4+2]-cycloaddition with **2a** in the presence of (*R*,*R*)-**Fe5**. All corresponding products **3ca**–**3ha** were obtained in generally high yields and enantioselectivities. Importantly, the cycloaddition protocol is easily amenable to scale-up and **3ha** was obtained with identical 92:8 er and slightly improved 80% yield when the reaction was performed at a 4.0 mmol scale. Catalyst (*S*,*S*)-**Fe7** showed a good performance when aryl-substituted branched dienes (**1b**,**1i**–**1k**) were used. Steric and electronic modifications at the aryl moiety of the substrate only resulted in negligible changes in the enantiomeric ratio (**3ia**–**3ka**). Structural elucidation of **3ka** by X-ray indicated that the absolute configuration of the cycloadducts obtained using (*S*,*S*)-**Fe7** is (*S*).[30] Notably, **Fe7** also promotes the cycloaddition of feedstock dienes, like isoprene (**1m**) or 1,3-butadiene (**1n**) with linear diene **2a**. In this respect, cyclo-
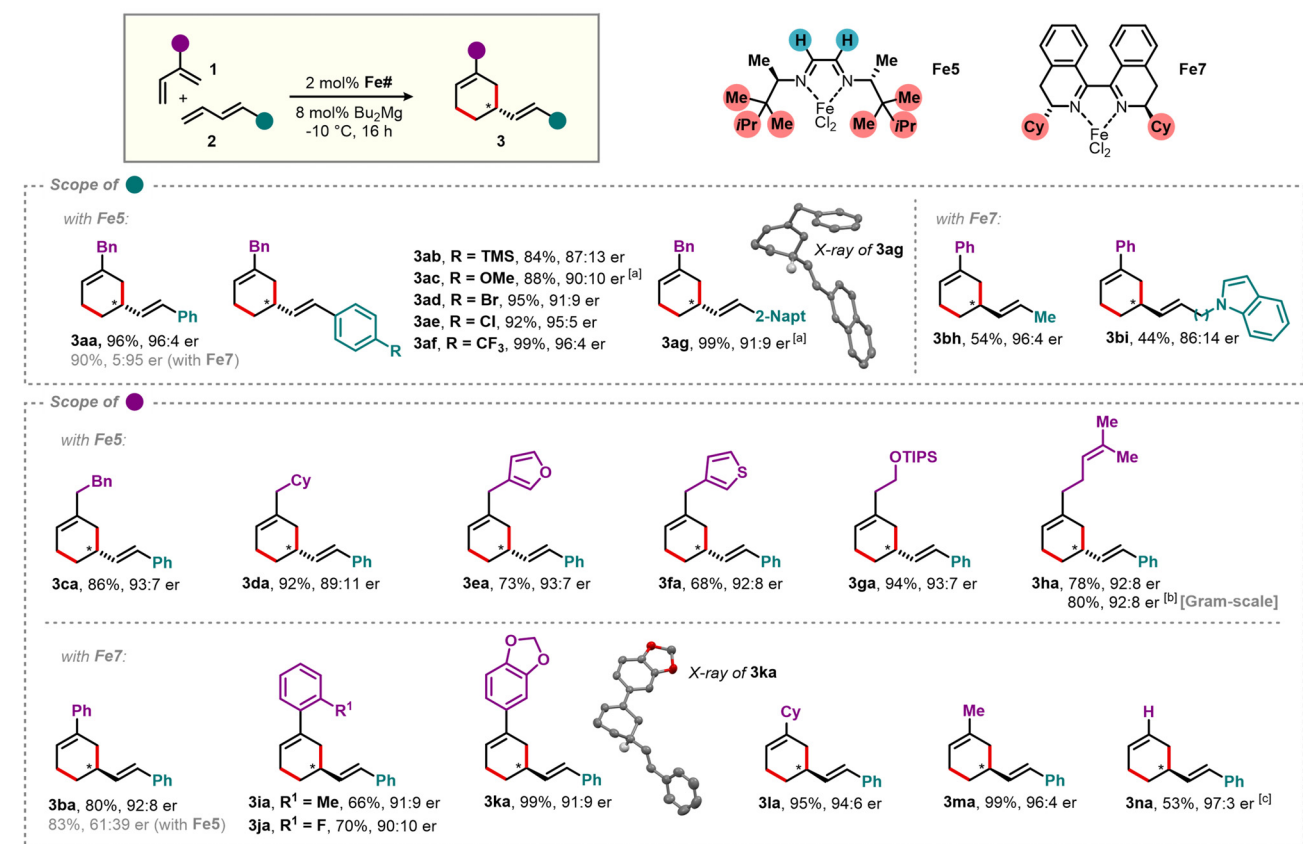
Scheme 2. Scope of the asymmetric Fe-catalyzed cross-[4+2]-cycloaddition. Conditions: 0.33 mmol **1**, 0.3 mmol **2**, 6 µmol (*R*,*R*)-**Fe5** or (*S*,*S*)-**Fe7**, 24 µmol Bu₂Mg (1 M in heptane) at −10°C for 16 h. [a] With 18 µmol (*R*,*R*)-**Fe5**, 72 µmol Bu₂Mg in PhMe (1 M). [b] 4.0 mmol scale. [c] At 25°C.
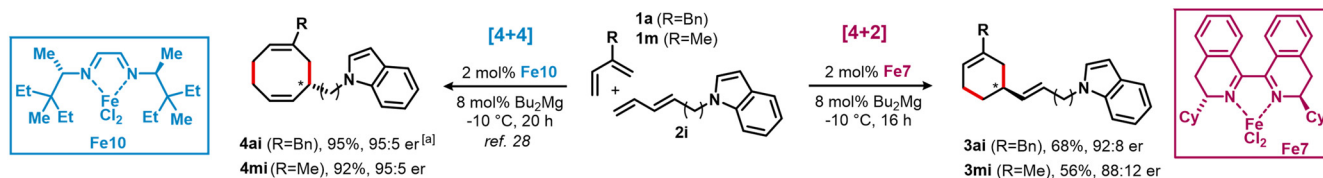
Scheme 3. Ligand-controlled switch between [4+4] and [4+2] cyclization modes. Conditions: 0.33 mmol **1**, 0.3 mmol **2**, 6 µmol **Fe7** or **Fe10**, 24 µmol Bu$_2$Mg (1 M in heptane) at −10 °C for 16 or 20 h. [a] With 4 mol% **Fe10**, 16 mol% Bu$_2$Mg for 40 h.

hexene **3na** was obtained in excellent 97:3 er and 53% yield, with some 1,5-cyclooctadiene (COD)[35] observed as by-product.

The chemoselectivity of the cyclization can be controlled by proper choice of the ligand (Scheme 3). For instance, using the same set of alkyl substituted dienes (**1a**, **1m** paired with **2i**), catalyst **Fe7** selectively induces the cross-[4+2]-cycloaddition yielding vinyl-cyclohexenes **3ai** and **3mi**. In contrast, cyclooctadienes **4ai** and **4mi** were exclusively formed using **Fe10** as the catalyst.[28]

To rationalize the effects of the catalyst on the chemoselectivity of the transformation, a working model for the mechanism could be formulated by combining previous findings from Chirik[26,27,36] and Lin[37] and our experimental observations (Scheme 4). An oxidative cyclization of in situ formed intermediate **Fe-I** and linear diene **2** connects both diene substrates. It may lead to the formation of seven-membered ferracycle **Fe-II** or alternatively nine-membered **Fe-III**. A subsequent reductive elimination would form, respectively cyclohexenes **3** or cyclooctadienes **4**. The "chemoselectivity switch" between [4+4] and [4+2] mode could plausibly result from increased steric congestion at the catalytic pocket, favoring **Fe-II** over **Fe-III**. In the case of a less favored reductive elimination from **Fe-II**, β-hydride

elimination could form **Fe-IV**. In turn, reductive elimination would yield hydrovinylation product **5**.

To gauge the influence of the (*E*/*Z*)-geometry of the linear diene **2** on the cycloaddition outcome, we independently reacted (*E*)-**2f** and (*Z*)-**2f** with **1a** in the presence of **Fe5** (Scheme 5A). Irrespectively of the starting double bond configuration, cyclohexene **3af** bearing an (*E*)-exocyclic double bond was obtained in both cases as the sole geometrical isomer in excellent yield. From a practical standpoint, this enables a convergent synthesis of (*E*)-products from mixtures of (*E*/*Z*)-diene substrates. However, notably different enantiomeric ratios for (*E*)-**3af** were observed. While (*E*)-**2f** resulted in the expected excellent er range of 96:4, substrate (*Z*)-**2f** was less selective yielding (*E*)-**3af** in 34:66 er. This finding suggests that the double bond geometry isomerization event to the more stable (*E*)-isomer has to occur after the enantiodetermining step. One can envision two possible scenarios: i) product isomerization by an independent off-cycle event; ii) isomerization during the catalytic cycle. Attempts to isomerize independently synthesized cyclohexane **6**[38] (a surrogate for (*Z*)-**3af**) under the standard reaction conditions failed (Scheme 5B). No change in the (*E*/*Z*)-ratio of **6** was detected, prompting us to discard the first hypothesis. Therefore, olefin isomerization likely is occurring on-cycle. Iron-mediated olefin isomerizations proceeding via alkene insertion/β-hydride elimination have been previously described.[39] The observation of hydrovinylation
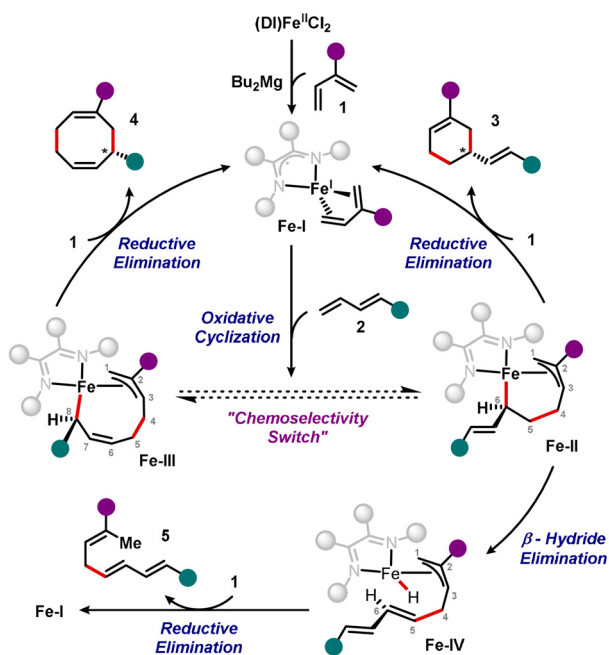
Scheme 4. Plausible mechanistic picture for the product landscape.
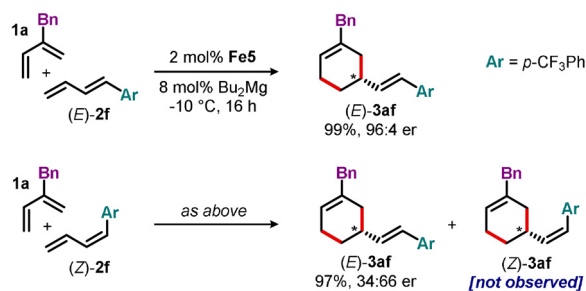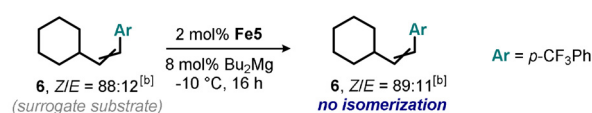
Scheme 5. Effect of the double bond geometry of **2f** on the reaction. [a] 0.33 mmol **1a**, 0.3 mmol (*E*)-**2f** or (*Z*)-**2f**, 6 µmol **Fe5**, 24 µmol Bu$_2$Mg at −10 °C for 16 h. [b] (*E*/*Z*)-Ratio determined by ^{19}F-NMR.

product **5ba** as side-product may suggest isomerization by this mechanism.

The largely different enantioselectivities from (*E*)-**2f** and (*Z*)-**2f** do exclude (*Z*)-to-(*E*) isomerization of the diene substrate. Likely, reductive elimination from intermediate **Fe-II** is not enantiodetermining. In this case, the same er for (*E*)-**3af** should have been observed irrespective of the linear diene olefin geometry. By exclusion principle, oxidative cyclization is likely the enantiodetermining step. This hypothesis is as well in line with Chirik's mechanistic investigations on related iron-catalyzed cross-[4+4]-cycloadditions,[27] for which stereoselective oxidative cyclization, followed by stereospecific allyl-isomerization/reductive elimination has been postulated.

In conclusion, we have developed an iron-catalyzed cross-[4+2]-cycloaddition of unactivated branched and linear dienes. The reaction operates at mild conditions and requires only minor solvent quantities. The illustrated process provides a very efficient and atom-economic access to 1,3-substituted vinyl-cyclohexenes, thus addressing a longstanding white spot in the asymmetric cycloaddition landscape. The development of a chiral *bis*-dihydroisoquinoline ligand class was essential to obtain excellent levels of chemo-, regio- and enantioselectivity for a broad range of unfunctionalized chiral cyclohexenes products.

Conflict of Interest

The authors declare no conflict of interest.

[1] G. W. Gribble in *Second Supplements to the 2nd Edition of Rodd's Chemistry of Carbon Compounds: A Modern Comprehensive Treatise* (Ed.: M. Sainsbury), Elsevier, Amsterdam, **1991**, pp. 375–445.

[2] P. Erasto, A. M. Viljoen, *Nat. Prod. Commun.* **2008**, *3*, 1193–1202.

[3] L. Jaenicke, D. G. Muellar, R. E. Moore, *J. Am. Chem. Soc.* **1974**, *96*, 3324–3325.

[4] G. S. R. Subba Rao, K. Srinivasa Rao, B. Ravindranath, *Tetrahedron Lett.* **1976**, *17*, 1019–1020.

[5] O. M. Ogba, N. C. Warner, D. J. O'Leary, R. H. Grubbs, *Chem. Soc. Rev.* **2018**, *47*, 4510–4544.

[6] G. Domínguez, J. Pérez-Castells, *Chem. Eur. J.* **2016**, *22*, 6720–6739.

[7] X. Liu, W. Zhang, Y. Wang, Z.-X. Zhang, L. Jiao, Q. Liu, *J. Am. Chem. Soc.* **2018**, *140*, 6873–6882.

[8] L. B. Smith, R. J. Armstrong, D. Matheau-Raven, T. J. Donohoe, *J. Am. Chem. Soc.* **2020**, *142*, 2514–2523.

[9] O. Diels, K. Alder, *Justus Liebig's Ann. Chem.* **1928**, *460*, 98–122.

[10] L. M. Joshel, L. W. Butz, *J. Am. Chem. Soc.* **1941**, *63*, 3350–3351.

[11] K. N. Houk, *J. Am. Chem. Soc.* **1973**, *95*, 4092–4094.

[12] H. Du, K. Ding in *Handbook of Cyclization Reactions* (Ed.: S. Ma), Wiley-VCH, Weinheim, **2010**, pp. 1–57.

[13] M. Lautens, W. Klute, W. Tam, *Chem. Rev.* **1996**, *96*, 49–92.

[14] R. S. Jolly, G. Luedtke, D. Sheehan, T. Livinghouse, *J. Am. Chem. Soc.* **1990**, *112*, 4965–4966.

[15] P. A. Wender, T. E. Jenkins, *J. Am. Chem. Soc.* **1989**, *111*, 6432–6434.

[16] L. McKinstry, T. Livinghouse, *Tetrahedron* **1994**, *50*, 6145–6154.

[17] S. R. Gilbertson, G. S. Hoge, D. G. Genov, *J. Org. Chem.* **1998**, *63*, 10077–10080.

[18] M. Newcomb, W. T. Ford, *J. Org. Chem.* **1974**, *39*, 232–236.

[19] L. M. Stephenson, R. V. Gemmer, S. Current, *J. Am. Chem. Soc.* **1975**, *97*, 5909–5910.

[20] I. Bauer, H.-J. Knölker, *Chem. Rev.* **2015**, *115*, 3170–3387.

[21] A. Fürstner, *ACS Cent. Sci.* **2016**, *2*, 778–789.

[22] B. Plietker, *Iron Catalysis in Organic Chemistry: Reactions and Applications*, Wiley-VCH, Weinheim, **2008**.

[23] M. Mohadjer Beromi, C. R. Kennedy, J. M. Younker, A. E. Carpenter, S. J. Mattler, J. A. Throckmorton, P. J. Chirik, *Nat. Chem.* **2021**, *13*, 156–162.

[24] M. D. Greenhalgh, S. P. Thomas in *Catalysis with Earth-Abundant Elements* (Eds.: U. Schneider, S. Thomas), The Royal Society Of Chemistry, London, **2020**, pp. 246–260.

[25] K.-U. Baldenius, H. tom Dieck, W. A. König, D. Icheln, T. Runge, *Angew. Chem. Int. Ed. Engl.* **1992**, *31*, 305–307; *Angew. Chem.* **1992**, *104*, 338–340.

[26] J. M. Hoyt, V. A. Schmidt, A. M. Tondreau, P. J. Chirik, *Science* **2015**, *349*, 960–963.

[27] C. R. Kennedy, H. Zhong, R. L. Macaulay, P. J. Chirik, *J. Am. Chem. Soc.* **2019**, *141*, 8557–8573.

[28] E. Braconi, A. C. Götzinger, N. Cramer, *J. Am. Chem. Soc.* **2020**, *142*, 19819–19824.

[29] T. Gaich, J. Mulzer in *Comprehensive Chirality* (Eds.: E. M. Carreira, H. Yamamoto), Elsevier, Amsterdam, **2012**, pp. 163–206.

[30] Deposition Numbers 2101842 (**Fe5**), 2101843 (**Fe7**), 2101844 (**Fe8**), 2101845 (**Fe9**), 2101846 (**3ag**), 2101847 (**3ka**) contain the supplementary crystallographic data for this paper. These data are provided free of charge by the joint Cambridge Crystallographic Data Centre and Fachinformationszentrum Karlsruhe Access Structures service www.ccdc.cam.ac.uk/structures.

[31] H. Seo, D. Hirsch-Weil, K. A. Abboud, S. Hong, *J. Org. Chem.* **2008**, *73*, 1983–1986.

[32] S. Miaskiewicz, J. H. Reed, P. A. Donets, C. C. Oliveira, N. Cramer, *Angew. Chem. Int. Ed.* **2018**, *57*, 4039–4042; *Angew. Chem.* **2018**, *130*, 4103–4106.

[33] L. Falivene, Z. Cao, A. Petta, L. Serra, A. Poater, R. Oliva, V. Scarano, L. Cavallo, *Nat. Chem.* **2019**, *11*, 872–879.

[34] P. Dierkes, P. W. N. M. van Leeuwen, *J. Chem. Soc. Dalton Trans.* **1999**, 1519–1530.

[35] H. Lee, M. G. Campbell, R. Hernández Sánchez, J. Börgel, J. Raynaud, S. E. Parker, T. Ritter, *Organometallics* **2016**, *35*, 2923–2929.

[36] V. A. Schmidt, C. R. Kennedy, M. J. Bezdek, P. J. Chirik, *J. Am. Chem. Soc.* **2018**, *140*, 3443–3453.

[37] Z. Zhang, J.-X. Zhang, F. K. Sheong, Z. Lin, *ACS Catal.* **2020**, *10*, 12454–12465.

[38] C. W. Cheung, F. E. Zhurkin, X. Hu, *J. Am. Chem. Soc.* **2015**, *137*, 4932–4935.

[39] X. Yu, H. Zhao, P. Li, M. J. Koh, *J. Am. Chem. Soc.* **2020**, *142*, 18223–18230.

Angew. Chem. Int. Ed. **2022**, *61*, e202112148 (5 of 5)

© 2021 The Authors. Angewandte Chemie International Edition published by Wiley-VCH GmbH